JOURNAL OF RESEARCH of the National Bureau of Standards
Vol. 89, No. 5, September-October 1984

Radio Propagation in a Coal Seam and the Inverse Problem

D. A. Hill
National Bureau of Standards Boulder, CO 80303

Accepted: July 17, 1984

The longwall method of mining in underground coal seams is very efficient in uniform seams, but coal seam anomalies can make the method unprofitable and unsafe. This paper describes the theoretical basis for detection of coal seam anomalies using medium frequency (MF) radio transmission over paths on the order of 200 m in length. The key to the method is the sensitivity of the attenuation rate of the coal seam mode of propagation to changes in the coal seam parameters, such as height or electrical conductivity. From a large number of transmission paths, the principles of tomography can be used to reconstruct an image of the seam.

Key words: attenuation rate; coal seam; geophysical tomography; linear equation inversion; loop antenna; medium frequency.

1. Introduction

Most coal seams are horizontally bedded deposits on the order of a few meters in thickness, and an ideal seam is fairly flat with little variation in thickness over a large region. In the longwall method of coal mining [1][1], two horizontal parallel entries separated by approximately 150 m are driven in the coal seam. The coal between the two entries is then mined out as the "longwall" retreats. The longwall method is very efficient for uniform coal seams, but coal seam anomalies can make the method unprofitable and unsafe. A remote sensing method that could detect coal seam anomalies would be extremely useful.

Seismic methods are currently being explored in coal seams [2], but their effectiveness is as yet undemonstrated. Underground radars using VHF (30 MHz-300 MHz) have been used for some short-range applications, but they do not have sufficient range [3] to probe the entire coal panel between the longwall entries. During the 1970s, it was found that communication between loop antennas using MF (300 kHz–3 MHz) was possible in coal seams for horizontal ranges up to several hundred meters [4,5]. The dominant mode of propagation at MF in coal seams is TM (transverse magnetic) with the magnetic field horizontally polarized. Because the electric field is primarily vertically polarized with only a small longitudinal component, the mode is nearly TEM (transverse electromagnetic) and is commonly referred to as the quasi-TEM mode or coal seam mode. And because the propagation constant of the quasi-TEM mode depends on the coal seam parameters (thickness and electrical properties), it should be a useful mode of propagation for remote probing of the coal seams.

This paper's purpose is to explore the theoretical feasibility of using MF radio transmission in remote sensing of coal seams, and its remaining sections are organized as follows. In section 2, the propagation constant and the field distribution are studied for a uniform coal seam. The dependence of the attenuation rate on the seam parameters is of particular importance. In section 3, the excitation of the TEM mode by a vertical loop (horizontal magnetic dipole) is analyzed. In section 4,

About the Author: D. A. Hill is an electronics engineer in NBS' Electromagnetic Fields Division.

[1]Figures in brackets indicate literature references at the end of this paper.

transmission through a longwall coal panel is examined and the question of how to process the transmission data is explored. This is an area where further work is required. In section 5, conclusions are presented, and areas for further work are suggested.

2. Attenuation Rate and Field Distribution for the Quasi-TEM Mode

The geometry for a uniform coal seam is shown in figure 1. The seam has thickness $2h$, and the coal permittivity and conductivity are ϵ_c and σ_c respectively. The permittivity and conductivity of the surrounding rock are ϵ_r and σ_r respectively. Free space permeability μ_0 is assumed everywhere.

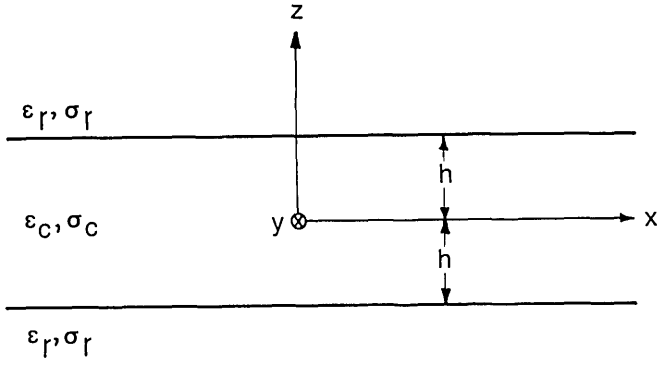

Figure 1—Geometry for a uniform coal seam of thickness $2h$.

The time dependence is $\exp(j\omega t)$, and it is suppressed throughout. The wavenumbers for the coal and rock, k_c and k_r, are given by

$$k_c=\omega\sqrt{\mu_0\epsilon_{cc}} \text{ and } k_r=\omega\sqrt{\mu_0\epsilon_{rc}}, \tag{1}$$

where $\epsilon_{cc}=\epsilon_c-j\,\sigma_c/\omega$

and $\epsilon_{rc}=\epsilon_r-j\,\sigma_r/\omega$.

The lowest order mode is transverse magnetic (TM), and for propagation in the x direction it has only an H_y magnetic field component. The mode equation for this lowest order mode has been given elsewhere [6,7], but we will derive it here because we need the resultant field expressions in the coal and in the rock. H_y must satisfy the following Helmholtz equation:

$$(\nabla^2+k_c^2)H_y=0,\ |z|<h$$

$$(\nabla^2+k_r^2)H_y=0,\ |z|>h. \tag{2}$$

The lowest order mode is even in z, and we also require that H_y is propagating in the x direction and satisfies eq (2). Thus we can write H_y in the coal ($|z|<h$) in the following form:

$$H_y=H_0\exp(-j\,k_c\,S\,x)\cos(k_c\,C\,z), \tag{3}$$

where $S^2+C^2=1$.

H_0 is an arbitrary constant, and S is a normalized propagation constant which must be determined from the mode equation. The fields are independent of y, and the x and z components of the electric field, E_x and E_y, are given by the following for $|z|<h$:

$$E_x=\frac{-1}{j\omega\epsilon_{cc}}\frac{\partial H_y}{\partial z} \text{ and } E_z=\frac{1}{j\omega\epsilon_{cc}}\frac{\partial H_y}{\partial x}. \tag{4}$$

Substituting eq (3) into eq (4), we obtain the following expressions for E_x and E_z:

$$E_x=-j\,C\,\eta_c\,H_0\exp(-j\,k_c\,S\,x)\sin(k_c\,C\,z),$$

$$E_z=-S\,\eta_c\,H_0\exp(-j\,k_c\,S\,x)\cos(k_c\,C\,z), \tag{5}$$

where $\eta_c=\sqrt{\mu_0/\epsilon_{cc}}$.

For $z>h$, H_y must satisfy the Helmholtz equation in eq (2). Also we require that H_y must decay as z goes to positive infinity. An appropriate form for H_y for $z>h$ is

$$H_y=A\exp(-j\,k_c\,S\,x)\exp(-j\,u\,z), \tag{6}$$

where $u=\sqrt{k_r^2-k_c^2\,S^2}$

and Im $(u)<0$.

A is an unknown constant, and Im denotes imaginary part. E_x and E_z are again determined from Maxwell's curl equation:

$$E_x=\frac{-1}{j\omega\,\epsilon_{rc}}\frac{\partial H_y}{\partial z}$$

$$=\frac{uA}{\omega\,\epsilon_{rc}}\exp(-j\,k_c\,S\,x)\exp(-j\,u\,z)$$

and (7)

$$E_z=\frac{1}{j\omega\,\epsilon_{rc}}\frac{\partial H_y}{\partial x}=\frac{-k_c\,S\,A}{\omega\,\epsilon_{rc}}\exp(-j\,k_c\,S\,x)\exp(-j\,u\,z).$$

Similar expressions for H_y, E_x, *and* E_z can be obtained for $z<h$ from the fact that H_y and E_z are even in z and E_x is odd in z.

At $z=h$, H_y and E_x must be continuous which leads to the following pair of equations:

$$H_0 \cos(k_c C h) = A \exp(-j u h),$$

$$-j C \eta_c H_0 \sin(k_c C h) = \frac{uA}{\omega \epsilon_{rc}} \exp(-j u h). \quad (8)$$

From the first equation A can be written

$$A = \frac{H_0 \cos(k_c C h)}{\exp(-j u h)}. \quad (9)$$

By substituting eq (9) into the second equation in eq (8), we obtain the following mode equation to be solved for C:

$$j k_c C \tanh(j k_c C h) + j u \epsilon_{cc}/\epsilon_{rc} = 0. \quad (10)$$

Equation (10) is consistent with earlier results [6-8], and is in a form which is easy to solve numerically. The solution of eq (10) by Newton's method [9] is detailed in the Appendix.

The reason that coal seams support a quasi-TEM mode quite effectively is that the coal conductivity σ_c is normally much smaller than the rock conductivity σ_r [4,7]. The propagation constant Γ of the quasi-TEM mode is given by

$$\Gamma = j k_c S = j k_c \sqrt{1-C^2}, \quad (11)$$

where Re $(\Gamma)>0$,

C is determined from Appendix eq (A-3) and Re indicates the real part. The attenuation rate of the coal seam is the easiest quantity to obtain from transmission measurements, and is given by 8.686 Re (Γ) in dB/m. Additional information is available from the phase velocity of the quasi-TEM mode, but phase measurements have not been attempted in coal seams.

In figure 2 we show the attenuation rate of the quasi-TEM mode as a function of frequency for the following parameters:

$\sigma_c = 10^{-4}\ S/m$, $\epsilon_c/\epsilon_0 = 6$, $\sigma_r = 10^{-1}\ S/m$, $\epsilon_r/\epsilon_0 = 15$, and $2h = 2$m.

The permittivities are normalized to the free space value ϵ_0. The computer code, written to generate the attenuation rate, was checked by comparing the results with those of Delogne [7], and in all cases agreed to graphical accuracy. As expected, the attenuation rate increases with frequency just as it does for a plane wave in an infinite rock medium. This indicates that the chosen frequency should be as low as possible to increase the range. However, there are two reasons for not choosing too low a frequency. For remote sensing, the resolution decreases as the frequency is decreased. Also, antenna efficiency decreases as the frequency is decreased. As a result of the tradeoff between attenuation rate and antenna efficiency, the maximum communication range between loop antennas in a coal seam was obtained for frequencies on the order of 500 kHz [5].

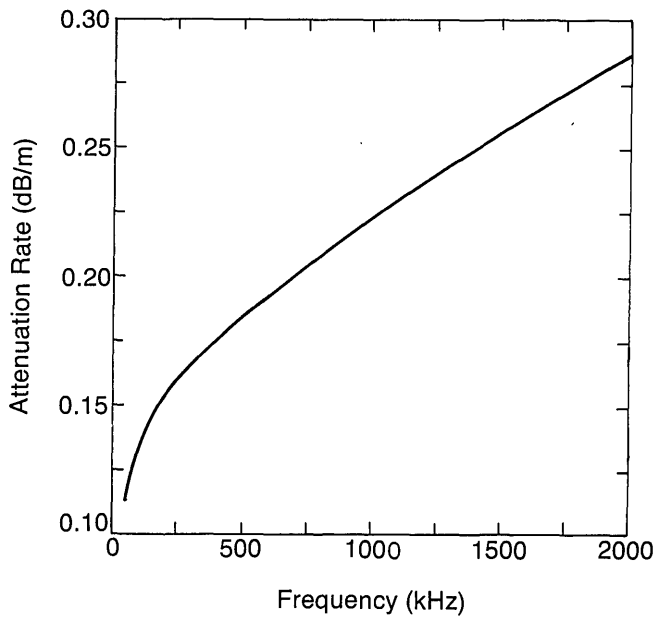

Figure 2—Attenuation rate as a function of frequency. Parameters: $\sigma_c = 10^{-4}$ S/m, $\epsilon_c/\epsilon_0 = 6$, $\sigma_r = 10^{-1}$ S/m, $\epsilon_r/\epsilon_0 = 15$, $2h = 2$m.

In figures 3–5, we show the attenuation rate as a function of various seam parameters for a frequency of 500 kHz. Since the goal is to detect changes in seam parameters from measurements of attenuation rate, it is desirable for the attenuation rate to be sensitive to changes in the seam parameters. The most important thing to detect in practical applications is a decrease in seam thickness $2h$. Figure 3 shows that the attenuation rate increases rapidly as thickness decreases below 1 m. This qualitative behavior can be predicted from Appendix eq (A-6). In figure 4 the attenuation rate is seen to increase as coal conductivity σ_c increases for both a plane wave and the quasi-TEM mode. The behavior of the attenuation rate as a function of rock conductivity σ_r is more complicated, as shown in figure 5. For large σ_r, the wall loss decreases as σ_r is increased as indicated by the second term in Appendix eq (A-6). However, as σ_r becomes small, more of the energy propagates in the rock, and the attenuation rate decreases as σ_r decreases.

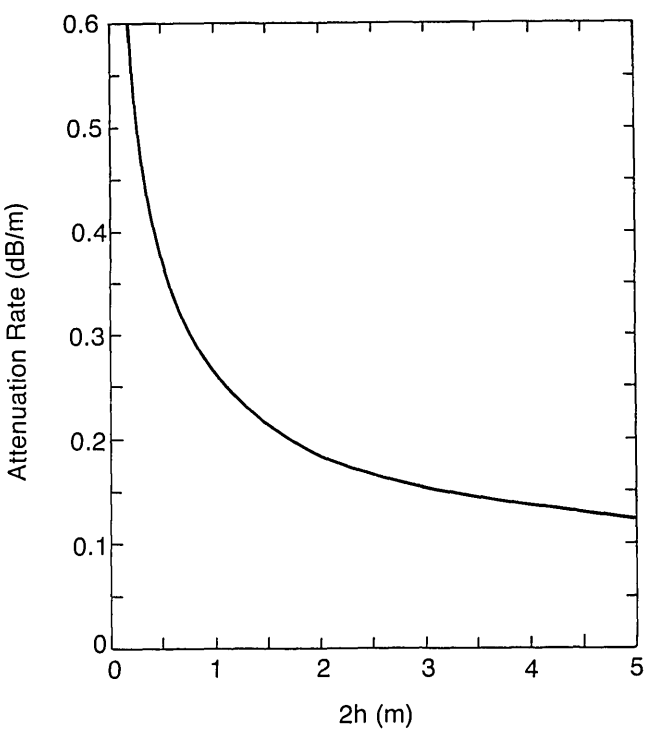

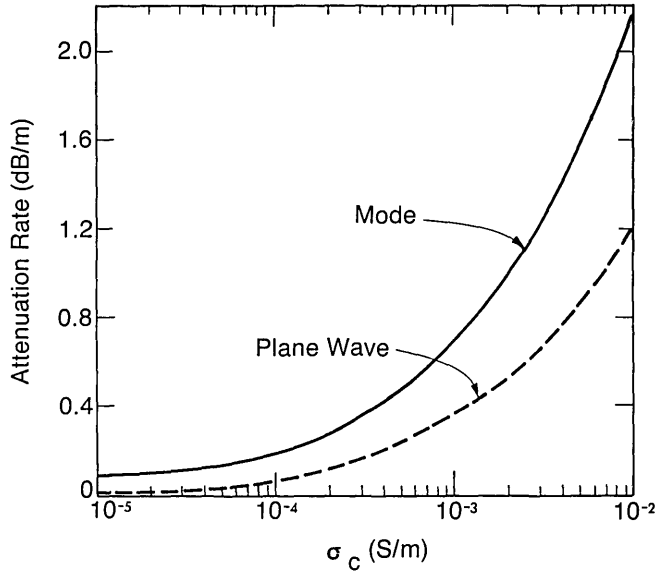

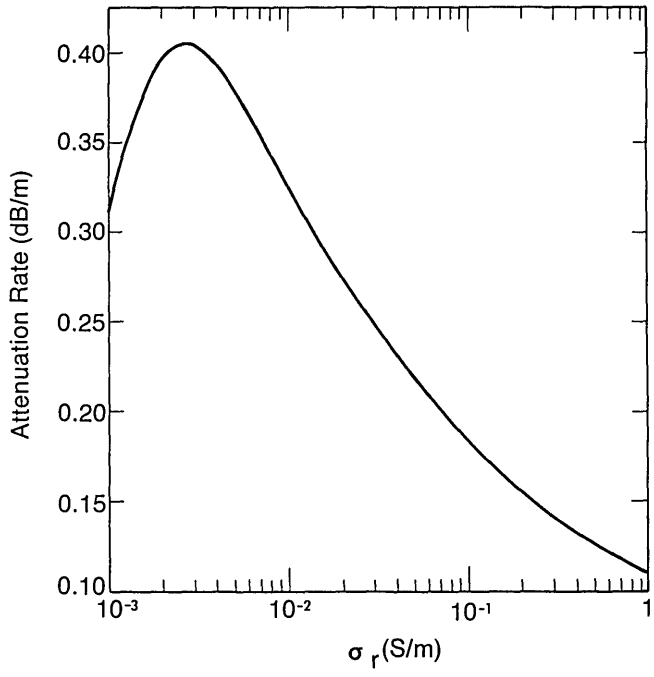

Figure 3-5—From above, clockwise: Attenuation rate as a function of seam thickness. Parameters: $f=500$ kHz, $\sigma_c=10^{-4}$ S/m, $\epsilon_c/\epsilon_0=6$, $\sigma_r=10^{-1}$ S/m, $\epsilon_r/\epsilon_0=15$. Next, attenuation rate for both a plane wave and the quasi-TEM mode as a function of coal conductivity. Parameters: $f=500$ kHz, $\epsilon_c/\epsilon_0=6$, $\sigma_r=10^{-1}$ S/m, $\epsilon_r/\epsilon_0=15$, $2h=2$m. Finally, attenuation rate as a function of rock conductivity. Parameters: $f=500$ kHz, $\sigma_c=10^{-4}$ S/m, $\epsilon_c/\epsilon_0=6$, $\epsilon_r/\epsilon_0=15$, $2h=2$m.

In figures 6–8 the electric and magnetic field distributions are shown for three different values of rock conductivity σ_r. The normalization field E_0 is the value of E_z at $z=0$ and is given by

$$E_0=\eta_c S H_0. \tag{12}$$

All field components decay exponentially in the rock ($z>h$), and the decay rate is most rapid for the largest value of σ_r. Inside the coal seam, H_y and E_z are the dominant field components, and they are nearly constant in z. Thus a vertical electric dipole or a horizontal magnetic dipole could be used to excite (or receive) the mode, and they would be insensitive to the vertical position. The horizontal electric field is zero at the center of the seam and is fairly small throughout the seam. Thus the mode is quasi-TEM. However, in the rock $|E_x|$ is larger than $|E_z|$ because E_z drops discontinuously to a small value in the rock. Thus the electric current flow is primarily horizontal in the rock. In addition to providing information on excitation of the quasi-TEM mode, the field distributions in figures 6–8 also indicate how anomalies in the seam will be illuminated.

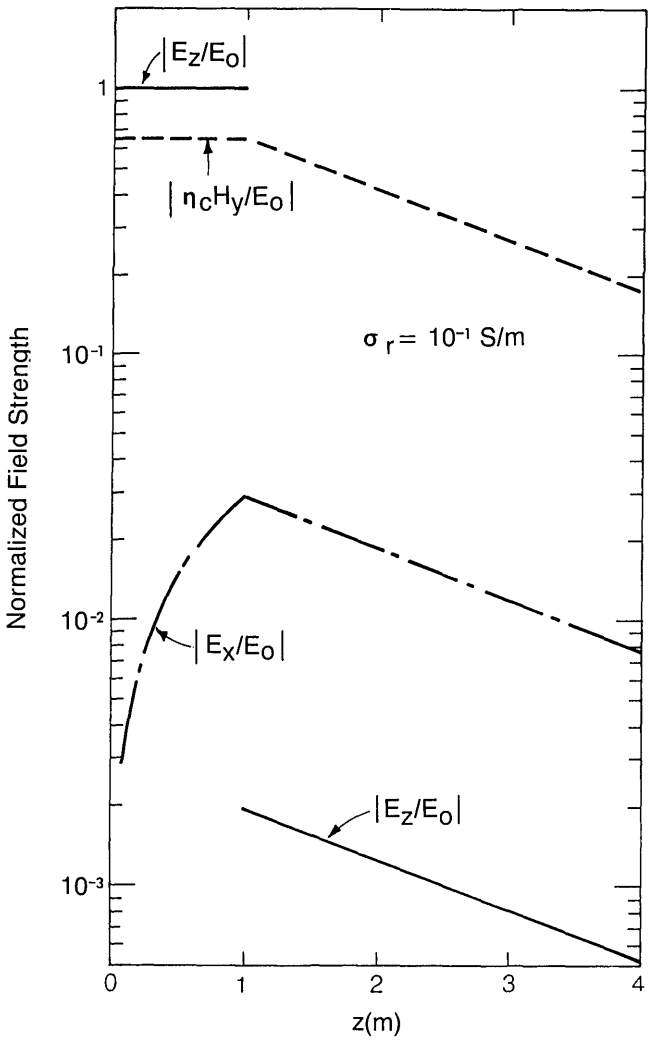

Figure 6—Electric and magnetic field distributions of the quasi-TEM mode. Parameters: $f=500$ kHz, $\sigma_c=10^{-4}$ S/m, $\epsilon_c/\epsilon_0=6$, $\sigma_r=10^{-1}$ S/m, $\epsilon_r/\epsilon_0=15$, $2h=2$m.

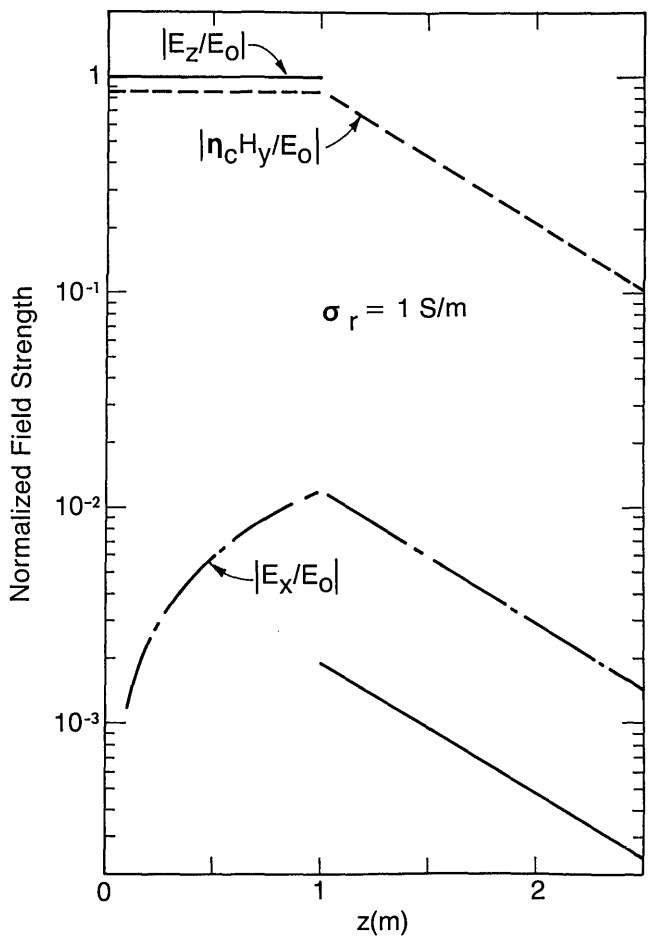

Figure 7—Electric and magnetic field distributions for a higher rock conductivity.

3. Excitation of the Coal Seam Mode by a Vertical Loop Antenna

From the field distributions in figures 6–8, it is clear that either a vertical electric dipole or a horizontal magnetic dipole will be effective in exciting the quasi-TEM mode. Short electric dipoles (or monopoles) located in or near a conducting medium are generally inefficient because of near-field losses [10-12]. The near-field losses are generally smaller for magnetic dipoles or small loops [11,13], because the dominant near field is the quasi-static magnetic field. Consequently loop antennas have been considered best for communication in coal seams [4,5]. In this section we analyze the excitation of the quasi-TEM mode by a horizontal magnetic dipole (a small vertical loop with its axis horizontal).

We consider a small loop of area A carrying a current I as shown in figure 9. The loop is centered on the z axis at $z=z_0$, and the loop axis is in the y direction. Thus the source can be considered a y-directed magnetic dipole of moment IA. This source radiates both a continuous spectrum of plane waves and a discrete spectrum of waveguide modes. For sufficiently large horizontal distances, the continuous spectrum can be ignored because it corresponds to highly attenuated waves traveling in the highly conducting rock walls. Also all higher order waveguide modes are highly attenuated because they are all well below cutoff. This is because $|k_c|2h$ is much less than unity at MF. Thus only the quasi-TEM mode which has no low frequency cutoff is significant at MF.

The excitation of the quasi-TEM mode has been considered by Delogne [7], and his result for the azimuthal component of the magnetic field H_ϕ is

$$H_\phi=\frac{k_c^2 IA}{2\pi h}\,\Lambda\cos(k_c C z)\cos(k_c C z_0)\,K_1(\Gamma\rho)\cos\phi,$$

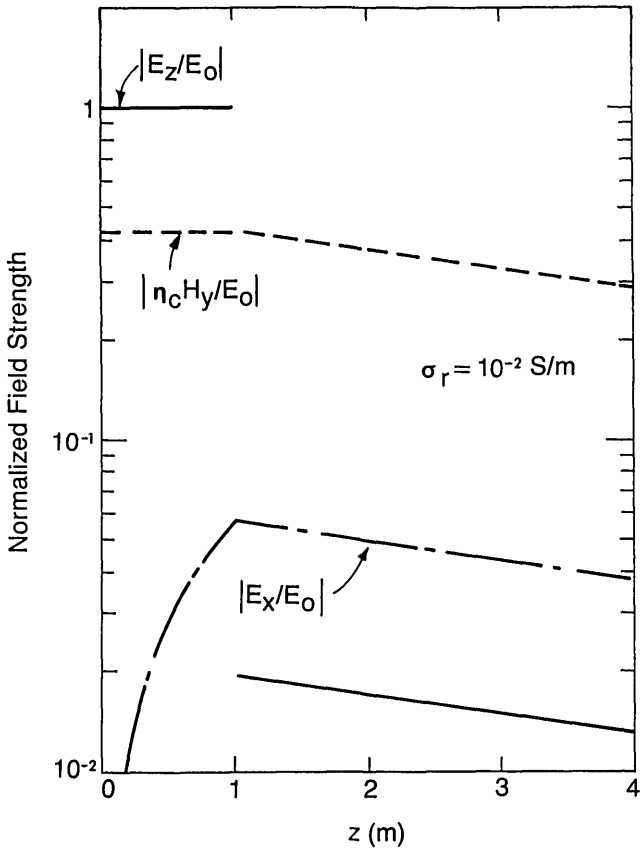

Figure 8—Field distribution for a lower rock conductivity.

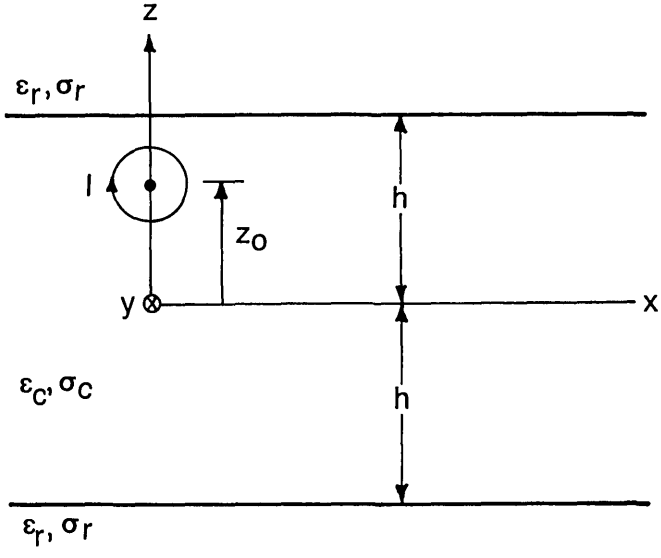

Figure 9—Vertical source loop (horizontal magnetic dipole) in a coal seam.

where $\cos\phi=\frac{x}{\rho}$, $\rho=\sqrt{x^2+y^2}$, (13)

$$\Lambda=\left[1+\frac{k_r^2-k_c^2}{k_r^2-k_c^2 C^2}\frac{\sin(k_c C\,2h)}{(k_c C\,2h)}\right]^{-1},$$

K_1 is a modified Bessel function [14], and C is determined from the solution of the mode eq (10). Equation (13) is valid when both the source and the field point are located in the coal seam ($|z|<h$ and $|z_0|<h$), and this is the usual case of interest. When $|\Gamma|\rho$ is large, we can replace $K_1(\Gamma\rho)$ by its asymptotic expansion [14]:

$$K_1(\Gamma\rho)\sim\sqrt{\frac{\pi}{2\Gamma\rho}}\exp(-\Gamma\rho). \tag{14}$$

Using eq (14), we can rewrite eq (13) as

$$H_\phi\sim H_i\frac{2\rho}{h}\sqrt{\frac{\pi}{2\Gamma\rho}}\,\Lambda\cos(k_c C z)\cos(h_c C z_0)\exp[-j k_c(S-1)\rho], \tag{15}$$

where

$$H_i=\frac{I A k_c^2}{4\pi\rho}\exp(-j k_c\rho)\cos\phi.$$

The reason for the normalization in eq (15) is that H_i is the far field of a magnetic dipole in an infinite coal medium for the case $z=z_0$. Note that the $\cos\phi$ factor leads to maximum in the plane of the loop ($y=0$) and nulls along the loop axis ($x=0$). The remaining factors yield the effect of the surrounding rock walls. The first factors involving ρ and h indicate that the coal seam mode has cylindrical spreading whereas H_i has spherical spreading. Λ relates to the excitation of the mode. The two cosine factors are the "height-gain" factors for the source and the observer within the seam. The exponential factor arises because the propagation constant of the mode is not the same as that of the infinite coal medium.

For the case where the rock conductivity is much greater than the coal conductivity ($|k_r|\gg|k_c|$), the expression in eq (15) simplifies considerably. In this case, C and S are given approximately by Appendix eqs (A-5) and (A-6):

$$C\simeq\sqrt{\frac{j}{k_r h}}\text{ and }S\simeq 1+\frac{1}{j2k_r h}. \tag{16}$$

Thus C is small, and S is close to unity. We assume that $k_c C h$ is small compared to unity, and thus the cosine factors are nearly unity:

$$\cos(k_c C z)\simeq\cos(k_c C z_0)\simeq 1. \tag{17}$$

This means that the height of the transmitter and receiver within the coal seam is not important, and this is consistent with the numerical results in figures 6–8. The exponential factor can be simplified from eq (16):

$$\exp\,[-j\,k_c\,(S-1)\rho] \simeq \exp\left(\frac{-k_c\,\rho}{2\,k_r\,h}\right). \qquad (18)$$

The excess attenuation over that of an infinite coal medium is given by eq (18), and is seen to be inversely proportional to that coal seam thickness $2h$. This is an important result in remote sensing of the seam height. The remaining factors in eq (15) can also be simplified from eq (16), and the result for H_ϕ is

$$H_\phi \simeq H_t \sqrt{\frac{\rho}{h}}\,\sqrt{\frac{\pi}{2j\,k_c\,h}}\,\exp\left(\frac{-k_c\,\rho}{2\,k_r\,h}\right). \qquad (19)$$

4. Interpretation of the Transmission Data

In longwall mining there are normally two parallel entries approximately 150 m apart, and these entries are accessible for radio transmission measurements. A logical measurement scheme is to step the transmitting and receiving loop antennas along the entries as shown in figure 10. If there are N transmitting and N receiving positions, then there are N^2 transmission measurements. The loops are assumed to have their axes in the y direction, and the received voltage v is proportional to H_x:

$$v = j\,\omega\,\mu_0\,A_r H_x, \qquad (20)$$

where $H_x = H_\phi \cos\phi$

and A_r is the area of the receiving loop.

There are many possible methods for interpreting the transmission data. Since the coal seam supports only a single mode at MF, the attenuation rate of the quasi-TEM mode is the most logical quantity to work with. If we assume that the coal seam parameters vary slowly, we can approximately neglect reflection and refraction and assume straight ray propagation as indicated in figure 10. In that case the magnitude of H_x for the i^{th} ray path can be approximately written:

$$|H_{xi}| \simeq \frac{H_t \cos^2\phi_i}{\sqrt{\rho_i}}\,\exp\left[-\int_0^{\rho_i} \alpha\,(x,y)\,d\rho\right], \qquad (21)$$

where H_t is a constant depending on the transmitting antenna and the coal seam parameters, $\alpha(x, y)$ is the attenuation rate in nepers/m and depends on x and y, ρ_i is the length of the i^{th} ray, and ϕ_i is the angle of the i^{th} ray with the x axis. The form of eq (21) is justified from the theory for the uniform coal seam in the previous section.

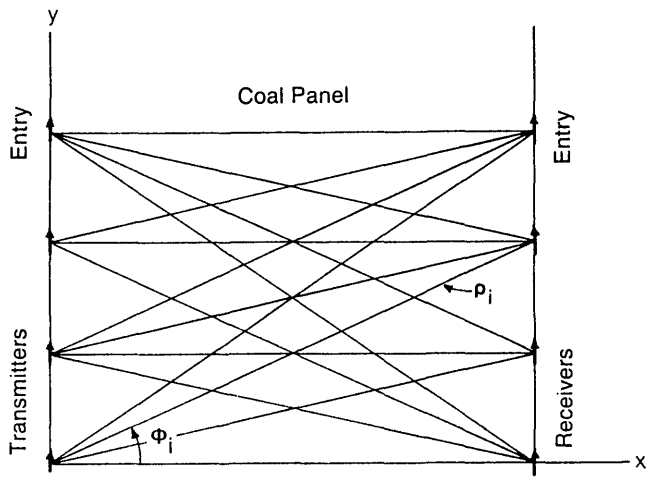

Figure 10—Top view of a longwall mine. The transmitting and receiving loops have their axes in the y direction and are moved along the parallel entries.

From eqs (20) and (21), the magnitude of the received voltage v_i for the i^{th} ray path can be written:

$$|v_i| \simeq \frac{V_0 \cos^2\phi_i}{\sqrt{\rho_i}}\,\exp\left[-\int_0^{\rho_i} \alpha\,(x,y)\,d\rho\right], \qquad (22)$$

where V_0 is a constant which depends on both antennas and the seam parameters. Taking the logarithm of both sides of eq (22), we have

$$\int_0^{\rho_i} \alpha\,(x,y)\,d\rho = \ln\frac{V_0 \cos^2\phi_i}{|v_i|\,\sqrt{\rho_i}}. \qquad (23)$$

In geophysical tomography [15-17], the usual approach is to divide the intervening region into some large number of cells over which α is assumed to be constant. In that case the path integral in eq (23) can be reduced to a sum, and eq (23) can be written

$$\sum_l D_{il}\,X_l = Y_i, \qquad (24)$$

where $Y_i = \ln\dfrac{V_0 \cos^2\phi_i}{|v_i|\,\sqrt{\rho_i}}$,

X_l equals the unknown attenuation rate α for the l^{th} cell, D_{il} equals the length of the i^{th} ray through the l^{th} cell as

shown in figure 11, and $|v_i|$ is the magnitude of the measured voltage for the i^{th} ray path. Since eq (24) applies to all rays, the total system of equations can be written in the following matrix forms:

$$[D_{il}]\,[X_l]=[Y_i]. \tag{25}$$

$[Y_i]$ is a column vector with N^2 elements corresponding to the N^2 transmission measurements in figure 10. The number of elements M in the unknown column matrix $[X_l]$ equals the number of cells, and normally M is chosen equal to or somewhat less than N^2.

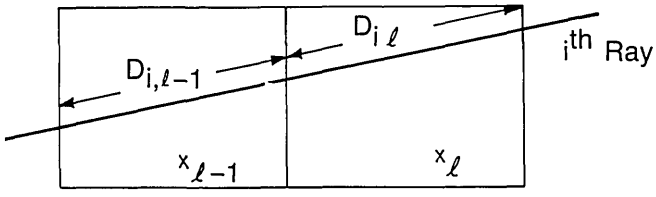

Figure 11—Geometry for the i^{th} ray. X_j is the attenuation rate in the j^{th} cell.

In theory $[X_l]$ could be determined from eq (25) by matrix inversion or pseudo-inversion:

$$[X_l]=[D_{il}]^{-1}\,[Y_i],\ M=N^2$$

or (26)

$$[X_l]=\left[[D_{il}]^T\,[D_{il}]\right]^{-1}\,[D_{il}]^T\,[Y_i],\ M>N^2,$$

where T indicates transpose.

In practice, the inversion of the linear equation in eq (25) has several difficulties. The values of $[Y_i]$ are not known exactly because $|v_i|$ contains noise and measurement error. Both the path integral model in eq (23) and the discrete version in eq (24) are approximate. Also, the system of equations in eq (25) may be very large. For example, if the antenna spacing is 5 m over a length of 150 m, then the number of equations is $30\times30=900$. In spite of these difficulties, there are numerous techniques which have been successfully applied to geophysical tomography problems [15-17]. Some of the popular methods and their acronyms are: algebraic reconstruction technique (ART) [18], simultaneous iterative reconstruction technique (SIRT) [19], and back projection technique (BPT) [20]. The description and application of these methods to geophysical tomography is well covered [16,17]. Since our system of equations for the coal seam geometry as described by eqs (24) and (25) is nearly identical to the equations for cross-borehole probing [15-17], the past work on geophysical tomography is directly applicable. The two differences are that the coal seam mode experiences cylindrical spreading rather than spherical spreading and that the unknown is the attenuation rate of the coal seam mode rather than the bulk attenuation of the medium. The cylindrical spreading results in the $\rho_i^{-1/2}$ factor in eq (24) rather than ρ_i^{-1} for spherical spreading.

Since the solution of eq (25) for $[X_l]$ yields the attenuation rate α for the l^{th} cell, there is a further question of what seam parameters actually produced that value of α. The attenuation rate α is given by

$$\alpha=-\mathrm{Im}\,(k_c\,S). \tag{27}$$

In general S depends on the seam parameters in a complicated manner via the mode eq (10). Even when the rock walls are highly conducting, α is fairly complicated:

$$\alpha\simeq-\mathrm{Im}\,(k_c)+\mathrm{Re}\left(\frac{k_c}{2\,k_r\,h}\right). \tag{28}$$

Since α in eq (28) depends on three parameters (k_c, k_r, and h), we cannot determine the three parameters from α. However, in some cases additional geologic information might be available. For example if the rock and coal properties are known and constant, the seam height can be obtained from:

$$2h\simeq\frac{\mathrm{Re}\,(k_c/k_r)}{\alpha+\mathrm{Im}\,(k_c)}. \tag{29}$$

If eq (28) is not valid, 2h can be obtained from a curve as in figure 3.

Even if it were not possible to determine the coal seam parameters, just the information that seam attenuation α changes in a region would be valuable to miners. Such a change would indicate that the seam is not uniform, and core drilling could be done in that area to provide further information. In fact, in many cases the full tomographic processing of the transmission data might be more complicated than necessary. In some cases, anomalous regions have been readily apparent from the measured data because the few rays which pass through the region have shown very high attenuation [21]. The anomalies have later been verified by drilling or mining into the anomalous region. High conductivity anomalies in copper mines have also been found by a similar ray analysis [22].

The conditions under which the straight ray tomographic approximation is valid have been discussed by Dines and Lytle [16], and similar conditions apply here if we replace the wavelength by guide wavelength and

the skin depth by the 1/e distance for the mode. Then the conditions become [16]:

$$\rho_i > \frac{1}{\mathrm{Re}\,(S\,k_c)}, \text{ for all } i,$$

and

$$-2\ \mathrm{Im}\,(S\,k_c) < \mathrm{Re}\,(S\,k_c). \tag{30}$$

The first condition is well satisfied at 500 kHz for $\rho_i > 100$ m. The second condition is only marginally satisfied at 500 kHz, but is better satisfied when either the frequency or the coal dielectric constant ϵ_c is increased. Even when eq (30) is satisfied, it is also necessary that the seam parameters vary slowly in order that the straight ray approximation is valid. Otherwise reflection and refraction occur, and they can be included, but only with significant increase in complexity [23]. When scattering becomes very important, even further changes in the processing are required [24], and in some cases it is useful to search for the scattering pattern of expected anomalies [25]. More experience with coal seam anomalies is necessary to determine the best method for processing data. There is also the possibility that phase information could be useful.

5. Conclusions

The feasibility of using the quasi-TEM mode at MF for remote sensing of coal seams has been studied. The mode has sufficient range for transmission between longwall entries which are normally separated by about 150 m. The attenuation rate is sensitive to the coal seam parameters (coal conductivity, rock conductivity, and seam thickness), as shown in figures 3–5. Thus the mode should be useful in sensing variations in these parameters. The mode can be excited efficiently by a vertical electric dipole or a vertical loop (horizontal magnetic dipole).

Transmission between vertical loops located in the two entries appears to be a useful method for probing the coal seam. Because a coal seam supports only a single mode which is nearly TEM, the system of linear equations to be solved is nearly identical to the system of equations in geophysical tomography. Thus the work which has been done on geophysical tomography for cross-borehole probing is directly applicable to the probing of coal seams. In some cases, such as a fault or washout of the seam, the seam properties change rapidly, and tomography is not valid; strong scattering and reflection occur, and some other type of processing is required. However, the transmission measurements will still show that the seam is not uniform, and this information might be sufficient for practical mining applications. The same difficulties occur for other geophysical tomography applications when strong scattering is present in either electromagnetic or seismic cases [25].

The author would like to thank Dr. Larry G. Stolarczyk for suggesting the use of MF radio transmission for remote sensing of coal seams.

References

[1] Murphy, J. N. and H. E. Parkinson. Underground mine communications. Proc. IEEE **66**: 26-50; 1978.

[2] Buchanan, D. J.; P. J. Jackson and R. Davis. Attenuation and anisotropy in coal seams. Geophys. **48**: 133-147; 1983.

[3] Cook, J. C. Radar transparencies of mine and tunnel rocks. Geophys. **40**: 865-885; 1975.

[4] Emslie, A. G. and R. L. Lagace. Propagation of low and medium frequency radio waves in a coal seam. Radio Sci. **11**: 253-261; 1976.

[5] Cory, T. S. Wireless radio transmission at medium frequencies in underground coal mines. Summary of measurements and expected system propagational effects. Workshop on Electromagnetic Guided Waves in Mine Environments: Boulder, CO; 1978.

[6] Wait, J. R. Note on the theory of transmission of electromagnetic waves in a coal seam. Radio Sci. **11**: 263-265; 1976.

[7] Delogne, P. *Leaky Feeders and Subsurface Radio Communication*. Stevanage, UK: Peter Perigrinus Ltd.; 1982, Sec. 2.6.

[8] Wait, J. R. *Electromagnetic Waves in Stratified Media*, 2nd ed. New York: Pergamon Press; 1970, Ch. VI.

[9] Hamming, R. W. *Numerical Methods for Scientists and Engineers*. New York: McGraw-Hill; 1973, Ch. I.

[10] Wait, J. R. Impedance characteristics of electric dipoles over a conducting half-space. Radio Sci. **4**: 971-975; 1969.

[11] Wait, J. R. and D. A. Hill. Impedance of an electric dipole located in a cylindrical cavity in a dissipative medium. Applied Phys. **11**: 351-356, 1976.

[12] Hill, D. A. and J. R. Wait. The impedance of dipoles in a circular tunnel with an axial conductor. IEEE Trans. Geosci. Electron. **GE-16**: 118-126; 1978.

[13] Wait, J. R. and K. P. Spies. A note on the insulated loop antenna immersed in a conducting medium. Radio Sci. J. Res. NBS **68D**: 1249-1250; 1964.

[14] Abramowitz, M. and I. A. Stegun, Eds. Handbook of mathematical functions. Natl. Bur. Stand. (U.S.) Handbook; 1964.

[15] Lager, D. L. and R. J. Lytle. Determining a subsurface electromagnetic profile from high-frequency measurements by applying reconstruction technique algorithms. Radio Sci. **12**: 249-260; 1977.

[16] Dines, K. A. and R. J. Lytle. Computerized geophysical tomography. Proc. IEEE **67**: 1065-1073; 1979.

[17] Radcliff, R. D. and C. A. Balonis. Reconstruction algorithms for geophysical applications in noisy environments. Proc. IEEE **67**: 1060-1064; 1979.

[18] Gordon, R. A tutorial on ART (algebraic reconstruction techniques). IEEE Trans. Nucl. Sci. **NS-21**: 78-93; 1974.

[19] Gilbert, P. Iterative methods for the three-dimensional reconstruction of an object from projections. J. Theor. Biol. **36**: 105-117; 1972.
[20] Kuhl, D. E. and R. Q. Edwards. Image separation radioisotope scanning. Radiology **80**: 653-662; 1963.
[21] Stolarczyk, L. G. Private communication; 1984.
[22] Rao, V. M. and I. B. R. Rao. The radio wave absorption technique in Mailaram copper mines, India. Geophys. **48**: 391-395; 1983.
[23] Radcliff, R. D. and C. A. Balanis. Electromagnetic geophysical imaging incorporating refraction and reflection. IEEE Trans. Antennas Propagat. **AP-29**: 288-292; 1981.
[24] Devaney, A. J. Geophysical diffraction tomography. IEEE Trans. Geosci. Remote Sensing **GE-22**: 3-13; 1984.
[25] Lytle, R. J.; E. F. Laine; D. L. Lager and D. T. Davis. Cross-borehole electromagnetic probing to locate high-contrast anomalies. Geophys. **44**: 1667-1676; 1979.

Appendix—Solution of Mode Equation

To solve eq (10) by Newton's method, we first define the function $f(C)$:

$$f(C)=j\,k_c\,C\tanh(j\,k_c\,C\,h)+\left(\frac{\epsilon_{cc}}{\epsilon_{rc}}\right)\sqrt{k_r^2-k_c^2(1-C^2)}. \tag{A-1}$$

The derivative of $f(C)$ with respect to C is

$$f'(C)=\frac{\partial f}{\partial C}=j\,k_c\tanh(j\,k_c\,C\,h)-k_c^2\,C\,h\,\mathrm{sech}^2(j\,k_c\,C\,h)$$

$$+j\,(\epsilon_c/\epsilon_r)k_c^2\,C/\sqrt{k_r^2-k_c^2(1-C^2)}. \tag{A-2}$$

If C_n is an n^{th} estimate of the solution to $f(C)=0$, then by Newton's method [8] the $n+1$ estimate is

$$C_{n+1}=C_n-\frac{f(C_n)}{f'(C_n)}. \tag{A-3}$$

The iteration in eq (A-3) is continued until the change in C is sufficiently small.

An initial estimate C_0 can be obtained by considering the perfectly conducting parallel plate case ($\epsilon_{rc}=\infty$). In this case, the second term in eq (A-1) is zero, and the solution is $C_0=0$. For large $\epsilon_{rc}/\epsilon_{cc}$, C_0 is not zero, but it is still small. Thus we can replace the tanh function by its argument:

$$j\,k_c\,C_0\,(j\,k_c\,C_0\,h)+j\,k_n\,\epsilon_{cc}/\epsilon_{rc}\simeq 0. \tag{A-4}$$

The solution to eq (A-3) is

$$C_0\simeq\sqrt{\frac{J}{k_r\,h}}. \tag{A-5}$$

Equation (A-5) is consistent with an earlier result from Wait [8], and we use it for our initial estimate in eq (A-3). Equation (A-5) can also be used to obtain an approximate propagation constant of the mode:

$$j\,k_c\,S\simeq j\,k_c\sqrt{1-C_0^2}\simeq j\,k_c(1-\tfrac{1}{2}\,C_0^2)$$

$$\simeq j\,k_c+\frac{k_c}{2\,k_r\,h}. \tag{A-6}$$

The first term $j\,k_c$ is the propagation constant of a plane wave in an infinite coal medium, and the second term is a correction to account for the finite conductivity of the surrounding rock.